An Adaptive Spatial Filtering Method for Multi-Channel EMG Artifact Removal During Functional Electrical Stimulation With Time-Variant Parameters

Xiaoling Chen, Yuntao Jiao, Dong Zhang, Ying Wang, Xinyu Wang, Yuqi Zang, Zhenhu Liang, and Ping Xie

***Abstract*— Removing the stimulation artifacts evoked by the functional electrical stimulation (FES) in electromyogram (EMG) signals is a challenge. Previous researches on stimulation artifact removal have focused on FES modulation with time-constant parameters, which has limitations when there are time-variant parameters. Therefore, considering the synchronism of muscle activation induced by FES and the asynchronism of muscle activation induced by proprioceptive nerves, we proposed a novel adaptive spatial filtering method called G-S-G. It entails fusing the Gram-Schmidt orthogonalization (G-S) and Grubbs criterion (G) algorithms to remove the FES-evoked stimulation artifacts in multi-channel EMG signals. To verify this method, we constructed a series of simulation data by fusing the FES signal with time-variant parameters and the voluntary EMG (vEMG) signal, and applied the G-S-G method to remove any FES artifacts from the simulation data. After that, we calculated the root mean square (RMS) value for both preprocessed simulation data and the vEMG data, and then compared them. The simulation results showed that the G-S-G method was robust and effective at removing FES artifacts in simulated EMG signals, and the correlation coefficient between the preprocessed EMG data and the recorded vEMG data yielded a good performance, up to 0.87. Furthermore, we applied the proposed method to the experimental EMG data with FES-evoked stimulation artifact, and also achieved good performance with both the time-constant and time-variant parameters. This study provides a new and accessible approach to resolving the problem of removing FES-evoked stimulation artifacts.**

***Index Terms*— Artefact removal, adaptive spatial filtering, EMG, functional electrical stimulation, G-S-G method.**

I. INTRODUCTION

FUNCTIONAL electrical stimulation (FES) is a neuromodulation technique that induces muscle activation to produce movements. It is commonly used in rehabilitation therapy to maintain and restore motor function after a stroke [1], [2], [3], [4], [5], [6], [7]. However, it is a great challenge to realize real-time close-loop control in the FES process [8], [9], [10], [11]. Although some studies based on electromyogram (EMG) signals have been initiated [12], [13], [14], [15], [16], several problems remain, such as how to remove the stimulation artifacts in EMG signals. Studies have shown that the stimulation artifacts in EMG mainly involve the initial spikes and M-waves [17], which generate more energy than that of the EMG signals in humans [18]. Therefore, there is a need to investigate various methodologies to remove stimulation artifacts in EMG. Researchers have begun to explore the removal of FES artifacts in EMG signals, such as the Blank Window [16], Filter [19], [20], [21] and Blind Source Separation (BSS) [22], [23], [24]. The Blank Window method is the most primitive method. It entails removing the FES artifacts by setting the values of the time period in which the FES artifacts concentrate at zero. However, despite the simplicity of this method in FES artifact removal, increasing the stimulus intensity also induces more artifacts in EMG [17], hindering artifact removal. In attempts to resolve the above

Manuscript received 15 December 2022; revised 28 June 2023 and 1 August 2023; accepted 29 August 2023. Date of publication 8 September 2023; date of current version 12 September 2023. This work was supported in part by the S&T Program of Hebei under Grant 21372005D and Grant 21372001D, in part by the National Natural Science Foundation of China under Grant U20A20192 and Grant 62076216, in part by the Natural Science Foundation of Hebei Province under Grant G2020203012, in part by the Cultivation Project for Basic Research and Innovation of Yanshan University under Grant 2021LGZD010, and in part by the Funding Program for Innovative Ability Training of Graduate Students of Hebei Provincial Department of Education under Grant CXZZSS2023043. *(Corresponding authors: Zhenhu Liang; Ping Xie.)*

This work involved human subjects or animals in its research. Approval of all ethical and experimental procedures and protocols was granted by the Yanshan University Ethical Review Committee and performed in line with the Declaration of Helsinki.

Xiaoling Chen and Ping Xie are with the Key Laboratory of Measurement Technology and Instrumentation of Hebei Province and the Key Laboratory of Intelligent Rehabilitation and Neuromodulation of Hebei Province, Institute of Electric Engineering, Yanshan University, Qinhuangdao, Hebei 066104, China (e-mail: xlchen@ysu.edu.cn; pingx@ysu.edu.cn).

Yuntao Jiao, Dong Zhang, Ying Wang, and Xinyu Wang are with the Key Laboratory of Measurement Technology and Instrumentation of Hebei Province, Yanshan University, Qinhuangdao, Hebei 066104, China (e-mail: 18730290302@163.com; NickFat@163.com; 834052699@qq.com; 694216849@qq.com).

Yuqi Zang is with the Key Laboratory of School of Public Policy and Management of Hebei Province, Yanshan University, Qinhuangdao, Hebei 066104, China (e-mail: yqzang@ysu.edu.cn).

Zhenhu Liang is with the Key Laboratory of Intelligent Rehabilitation and Neuromodulation of Hebei Province, Institute of Electric Engineering, Yanshan University, Qinhuangdao, Hebei 066104, China (e-mail: zhl@ysu.edu.cn).

Digital Object Identifier 10.1109/TNSRE.2023.3311819

problems, some researchers have used filters to remove stimulation artifacts in EMG signals. For example, Rune Thorsen et al. used digital comb filters to suppress the spurious harmonics induced by FES [25]. Additionally, Muraoka et al. proposed multiple band-pass filters to suppress stimulation artifacts [18]. Although these methods can preserve EMG information after denoising in some slow movements, they have limitations for high-intensity motions. The BSS technology, as a powerful methodology for separating the source from the mixtures to obtain a series of components with statistical independence, provides a new method for removing FES artifacts. Two classical methods, empirical mode decomposition (EMD) and independent component analysis (ICA), have been widely applied. For example, Rakesh used EMD with Notch filtering to eliminate stimulation artifacts in EMG data [23]. Also, Zhou et al. devised a new method to extract EMG signals contaminated by FES under time-varying parameters [26]. In the case of a fixed stimulation frequency, this method can produce a superior effect in removing stimulation artifacts. However with this method, it takes a long time to parse the signal. Especially for FES-evoked harmonics with time-variant parameters, this method's real-time performance is limited.

In recent years, template subtraction has been widely used to remove FES artifacts [27]. This method utilizes the similarity principle of waveforms between stimulation artifacts under the same parameters to realize artifact removal. For example, Yeom et al. proposed an Adaptive Gram-Schmidt Filter (AGSF) algorithm for stable real-time estimation of continuous stimulation [28]. Li et al. proposed a strategy combining blanking and template subtraction methods to suppress stimulation artifacts in an EMG-driven closed-loop FES system [27]. However, the above methods can only handle fixed-parameter stimulation artifacts, but not variable-parameter artifacts. Additionally, the amplitude, spectrum and shape of the M-wave can change with muscle fatigue, affecting the removal efficiency of template subtraction. The disadvantages of this approach are that stimulation artifacts are difficult to manage under variable parameters, and the initial spikes are difficult to remove [15]. To address this issue, Zhu et al. proposed a new DBGS method to remove the stimulation artifacts of time-variant parameters in real-time. However, the DBGS method is limited by the length of the data. Therefore, a new method which is suitable for real-time analysis of FES artifacts with time-varying parameters is needed.

The main contribution of this study is to propose a new adaptive spatial filtering method, defined as the G-S-G method, which combines the G-S algorithm with the Grubbs criterion for removing the multi-channel EMG artifact during FES with time-variant parameters. To this end, we created a set of simulation data by fusing the FES artifacts with time-variant parameters and the voluntary EMG (vEMG) signals, and applied the G-S-G method to remove any FES artifacts from the simulations. After that, we calculated the root mean square (RMS) value for both preprocessed simulation data and vEMG data, and then compared them. Furthermore, we applied the proposed method to experimental EMG data with FES-evoked stimulation artifacts. This study provides a new approach to the issue of removing FES-evoked stimulation artifacts.

II. Materials And Methods

A. Subjects

Eight healthy controls (mean age 25±5 years; mean height 69.3±12.8kg; mean weight 171.8±6.6cm; 5 males) without any history of neurological disease were enrolled in the study. Participants were tested according to the Oldfield questionnaire [29]. This experiment complied with the Declaration of Helsinki and was approved by the Yanshan University Ethical Review Committee. All participants gave informed consent, and none of the subjects had previous experience with similar experiments.

B. Experimental Paradigm

The experiments were conducted in an electromagnetically shielded and dimly lit room. All participants were dressed in comfortable attire and performed elbow flexion with their left hand, following the instructions of the target task (Figure 1(A)). Figure 1(B) illustrates the placement of the EMG electrodes on both sides of the muscle belly, as well as the positioning of FES electrodes along the direction of the muscle fibers. The distance between the EMG electrodes is 4 cm, and the FES electrodes were symmetrically placed with an 8 cm distance between them. And the upper arm is at an angle of 150° to the forearm (Figure 1(C)). The experimental flow is depicted in Figures 1(D)-(F).

Considering the effect of the stimulation parameters on the EMG signal, we focused on the stimulus frequency and stimulus intensity. For this, we designed five tasks: (i) voluntary EMG (vEMG) recording during elbow flexion without FES (Figure 1(D)), (ii) EMG recording with a time-constant parameter FES (tc-FES) during elbow flexion (Figure 1(E-e1)), (iii) EMG recording with tc-FES when there was no action (Figures 1(E-e2)), (iv) EMG recording with time-variant parameter FES (tv-FES) during elbow flexion (Figures 1(F-f1)), and (v) EMG recording in conjunction with tv-FES during periods of inactivity (Figures 1(F-f2)). To record EMG data without FES artifacts, we developed a type (i) task consisting of 4 repetitive trials, and each trial had 4s relaxation and 3s elbow flexion. To obtain EMG data with tc-FES artifacts, we designed the type (ii) task to perform the same actions as task (i). Unlike in task (i), in the type (ii) task, we added the FES stimulation with several time-constant parameters with all of the frequency-intensity combinations. The parameter combinations are shown in Figure 1(E). We performed the task (ii) in each time-constant frequency-intensity combination. Meanwhile, we also designed a set of control tasks that only used the tc-FES artifacts described in the type (iii) task. Additionally, we developed task (iv) as the same as the actions in type (i) to record EMG data with tv-FES artifacts. Unlike the type (ii) and (ii) tasks, in the type (iv) task, we added FES stimulation with several time-variant parameters, which are listed in Figure 1(F). We performed the type (iv) task along a series of time-variant frequency-intensity combinations with intervals of 2 s. We also designed a set of control tasks with only time-variant parameter FES artifacts, as described in the type (v) task. During the experiment, each

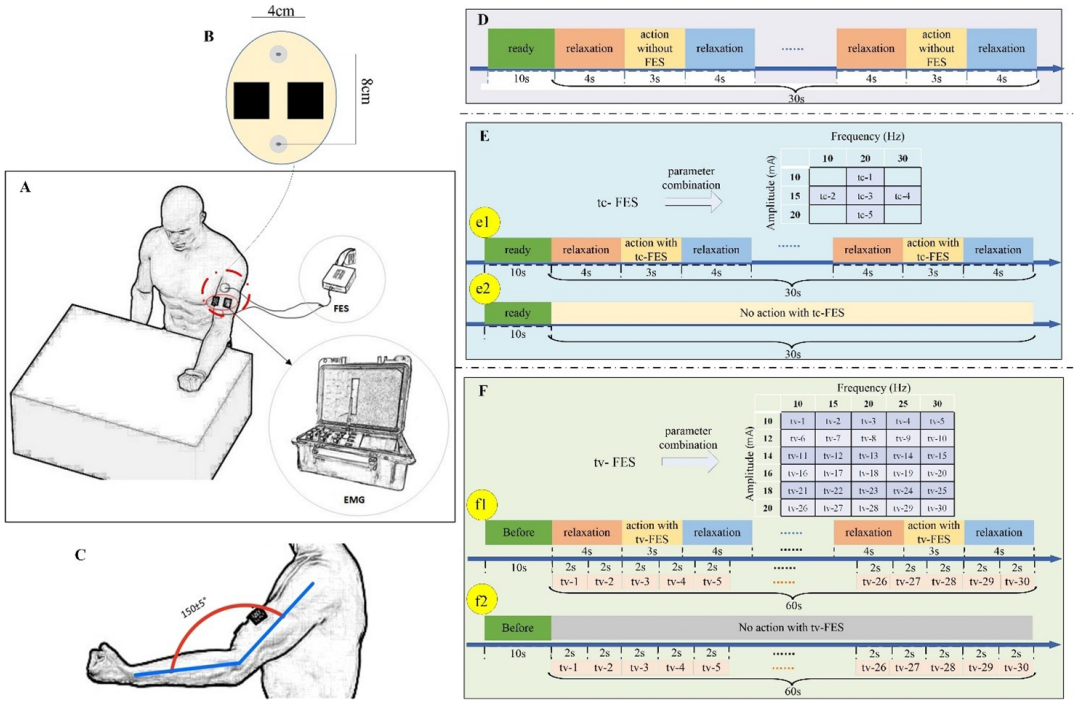

Fig. 1. Experimental paradigm: (A) schematic diagram of the experiment; (B) position of the EMG and FES electrodes; (C) schematic diagram of the target action (D) for (i) type of task: EMG signal recording when performing the upper limb action without FES, (E-el) for (ii) type of task: EMG signal recording when performing the action with tc-FES (E-e2) for (iii) type of task: EMG signal recording when there is no action with tc-FES. (F-f1) for (iiv) type of task: EMG signal recording when performing the action with tv-FES (F-f2) for (v) type of task: EMG signal recording when there is no action with tv-FES.

subject had to rest for 20 minutes between each task to avoid fatigue.

C. EMG Data Recording and Reconstruction

During the experiment, we recorded dual-channel EMG data from the biceps brachii muscle using the Trigno™Wireless EMG system (Delsys Inc, Ustimulation artifact) [30]. Before the electrode application, we cleaned the skin surface with alcohol. Figure 1(B) shows the distance between the two centers of the electrodes. At the same time, we also placed the FES electrodes next to the muscle, as shown in Figure 1(B). EMG data was amplified (1000), bandpass filtered (0.5-200Hz) and digitized (2000Hz). We recorded EMG data according to the above task types shown in Figure 1(D-F), respectively. In this study, we used EMG data in type (i), (iii) and (v) tasks to reconstruct the simulation EMG data to validate the proposed method. Then, we used this method to remove any FES artifacts from the raw EMG data for both the (ii) and the (iv) type tasks. To differentiate the EMG data from the five task types, we simplified the EMG signal types, as shown in Table I.

TABLE I
SIMPLIFICATION FOR ALL TYPES OF EMG SIGNAL

Abbreviation	Types of EMG Signal
vEMG	voluntary EMG data without FES artifacts
FES-EMG	EMG data with FES artifacts
FES-sEMG	simulation EMG data with FES artifacts
tc-FES	time-constant parameters FES artifacts
tv-FES	time-variant parameters FES artifacts
tc-FES-EMG	EMG data with time-constant parameters FES artifacts
tv-FES-EMG	EMG data with time-variant parameters FES artifacts
tc-FES-sEMG	simulation EMG data with time-constant parameters FES artifacts
tv-FES-sEMG	simulation EMG data with time-variant parameters FES artifacts

D. An Adaptive Spatial Filtering

The primary noises in EMG are initial spikes and M-waves, which are caused by FES and have serious negative effects on EMG data. Considering the correlation and synchronization of the stimulation artifacts in multichannel EMG [31], [32], we proposed a novel adaptive spatial filtering method, defined as the G-S-G method. It combines the G-S algorithm [28] with the Grubbs criterion [33] to remove both the initial spike and the M-waves in the EMG signals. Before that, we filtered raw EMG signals with a 20-200 Hz passband using a zero-phase-shift filter to reduce the high-frequency noise and low-frequency drift. Then we introduced a non-overlapping sliding window [34], [35] with window size T to divide the multichannel EMG data $X = \{x_1, x_2, \cdots, x_i, \cdots, x_M\}$ with data length L into a series of segments as follows:

$$X = \{X_1, X_2, \cdots, X_j, \cdots, X_N\} = \begin{Bmatrix} x_{1,1}, & x_{1,2}, \cdots, & x_{1,j}, & \cdots, x_{1,N} \\ x_{2,1}, & x_{2,2}, \cdots, & x_{2,j}, & \cdots, x_{2,N} \\ \vdots & \vdots & \vdots & \vdots \\ x_{i,1}, & x_{i,2}, \cdots, & x_{i,j}, & \cdots, x_{i,N} \\ \vdots & \vdots & \vdots & \vdots \\ x_{M,1}, & x_{M,2}, \cdots, & x_{M,j}, & \cdots, x_{M,N} \end{Bmatrix} \quad (1)$$

where the variates i ($i = 0, 1, \cdots, M$) and j ($j = 0, 1, \cdots, N$) were the index for the EMG channels and the sliding window, respectively, and M and N indicated how many channels and windows there were, respectively. The vector $x_{i,j}$ denotes the EMG data in the ith channel and jth window. Subsequently, we analyzed the vector $x_{*,j}$ in the jth window according to the following formula [28]:

$$\vec{\varepsilon}^{0}_{*,j} = x_{*,j} \tag{2}$$

$$w^{k}_{*,j} = \frac{\vec{\varepsilon}^{kT}_{*,j} \cdot \vec{\varepsilon}^{k}_{M-k,j}}{\left\| \varepsilon^{k}_{M-k,j} \right\|} \tag{3}$$

$$\vec{\varepsilon}^{k+1}_{*,j} = \varepsilon^{k}_{*,j} - w^{k}_{*,j} \cdot \vec{\varepsilon}^{k}_{M-k,j} \tag{4}$$

$$y_{*,j} = \vec{\varepsilon}^{k+1}_{*,j} \tag{5}$$

where k ($k = 0, 1, \cdots, M-1$) represented the order of the algorithm, and $*$ indicated one-channel EMG data. The variate $\vec{\varepsilon}^{k}_{*,j}$ denoted one-channel EMG data in the jth window after the kth order algorithm, while $w^{k}_{*,j}$ was the corresponding coefficient. After going through all channels in the jth window, we could remove the M-waves and most of the initial spikes, and obtain an EMG signal in the jth window $Y_j = \left\{ y_{1,j}, y_{2,j}, \cdots, y_{i,j}, \cdots, y_{M,j} \right\}$. After that, we needed to remove any outlier values. Thus, we first rectified the EMG data Y_j in the sliding window, and then applied the Grubbs criterion to identify and reject any outliers sequentially, and further remove any initial spikes. The specific steps are as follows:

$$Z_j = \left| Y_j \right| \tag{6}$$

After that, we calculated the G value for each g point in the ith channel in the jth segment window. The formula is as follows:

$$G_{i,j,g} = \frac{\left(z_{i,j,k} - \bar{z}_{i,j} \right)}{\hat{z}_{i,j}} \tag{7}$$

where k is the sequence number of the measurement point; $\bar{z}_{i,j}$ and $\hat{z}_{i,j}$ were the average value and standard deviation in the ith channel and jth window, respectively. Next, we needed to decide whether this was an outlier at this point. Typically, we would set a threshold G_p. if $G_{i,j,g} > G_p$, and the value at point g was abnormal. However, before this, we judged weather the data had been derived from the muscle activation by RMS values. If so, we then set a greater G_p value, defined as G_{p1}; if not, we set a lower G_{p2} value. In our study, considering that the data length of the slide window was 100, we set the G_{p1} as 0.1 and the G_{p2} as 0.05. If the value at this point was abnormal, we set the outliers to zero in dataset Y_j without rectification, and obtained the multichannel EMG data in the jth window $\bar{Y}_j = \left\{ \bar{y}_{1,j}, \bar{y}_{2,j}, \cdots, \bar{y}_{i,j}, \cdots, \bar{y}_{M,j} \right\}$.

After that, we used the band-pass filter to remove any harmonic interference and obtain the $S_j = \left\{ s_{1,j}, s_{2,j}, \cdots, s_{i,j}, \cdots, s_{M,j} \right\}$ in the jth window. The same process was suitable for the other segments, and we obtained the preprocessed EMG data set as follows:

$$S = \left\{ S_1, S_2, \cdots, S_j, \cdots, S_N \right\} = \begin{Bmatrix} s_{1,1}, & s_{1,2}, \cdots, & s_{1,j}, \cdots, & s_{1,N} \\ s_{2,1}, & s_{2,2}, \cdots, & s_{2,j}, \cdots, & s_{2,N} \\ \vdots & \vdots & \vdots & \vdots \\ s_{i,1}, & s_{i,2}, \cdots, & s_{i,j}, \cdots, & s_{i,N} \\ \vdots & \vdots & \vdots & \vdots \\ s_{M,1}, & s_{M,2}, \cdots, & s_{M,j}, \cdots, & s_{M,N} \end{Bmatrix} \tag{8}$$

The signal processing flow is shown in Figure 2. Figure 2(A) shows a flow chart of the G-S-G algorithm, Figures 2(B)-(F) show a diagram for the G-S-G method.

E. Evaluation Indices

To verify the effectiveness of the G-S-G method in removing FES artifacts, we introduced root mean square (RMS) [26], [27] to quantify the denoised EMG signals. If the length of the EMG data is L, the RMS value of each EMG channel after denoising in each segment is calculated as follows:

$$RMS_{i,j} = \sqrt{\frac{\sum_{t=1}^{T} s^2_{i,j,t}}{T}} \tag{9}$$

where $s_{i,j,t}$ is the t point in the ith channel of the jth segment. T is the window length, $RMS_{i,j}$ indicates the RMS values in the ith channel in the jth segment. After that, we obtained the series $RMS_i = \left\{ RMS_{i,1}, RMS_{i,2}, \cdots, RMS_{i,N} \right\}$ for the ith channel. Next, we calculated the correlation coefficient (r) of the RMS values between the de-noising EMG data and the vEMG data by Pearson correlation analysis. The greater the coefficient r, the better the preprocessing effect. To evaluate the robustness of the G-S-G algorithm to FES artifact under different parameters, we calculated the signal-to-noise ratio (SNR).([36] for each channel of the synthetic signal as follows:

$$SNR = 10 \lg \frac{\sum V^2}{\sum (H - V)^2} \tag{10}$$

where H represents the synthesized signal after algorithm processing, V represents the original uncontaminated EMG signal.

For real signals, it is not possible to obtain the original uncontaminated EMG signal. Therefore, we took the processed non-activity segments as noise and calculated the SNR of the signal by comparing it with the activity segments as follows.

$$SNR = 10 \lg \frac{\sum (R_b)^2}{\sum (R_a)^2} \tag{11}$$

where R_a represents the non-activity segments and R_b represents the activity segments.

III. Results

A. Performance Test for the G-S-G Method

We mainly utilized the computation libraries such as NumPy, SciPy, and Pandas in Python environment for data processing. We also employed the Excel software to plot

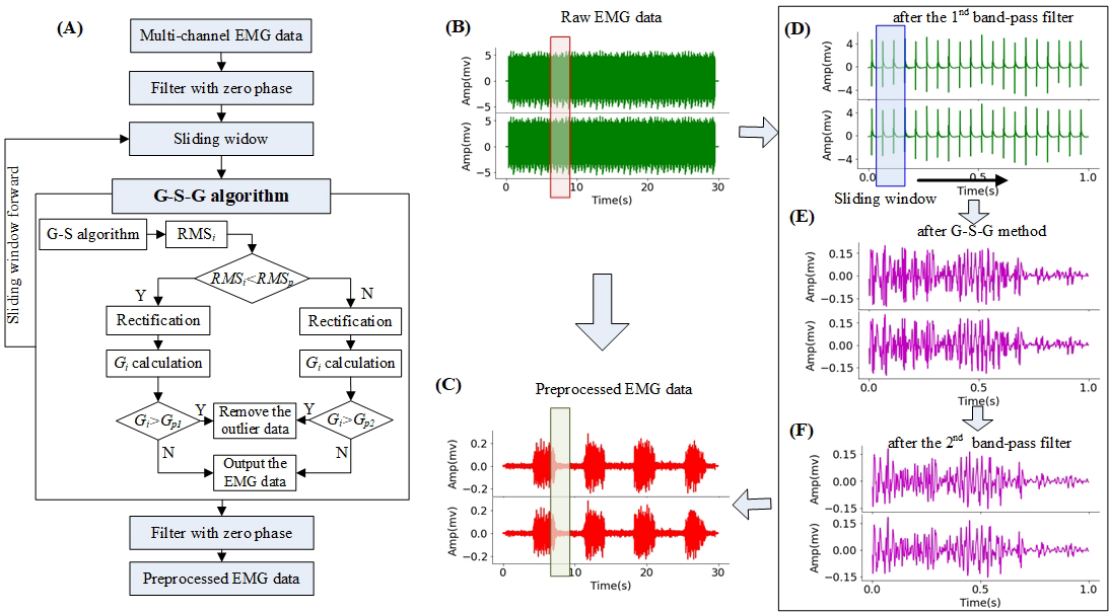

Fig. 2. Flow chart of the G-S-G algorithm. (A) is the flow chart of the G-S-G algorithm. (B)-(F) show the diagram for each step of the G-S-G method.

some visual figures. This platform configuration meets the requirements of our algorithm and ensures the accuracy and efficiency of computations.

1) Results for Tc-FES-sEMG: Construction for simulation EMG data with time-constant parameters FES artifacts:

To verify the effectiveness of the G-S-G method, we first fused the vEMG signal and the tc-FES artifacts at a ratio of 1:1 to construct simulated EMG data with FES artifacts with time-constant parameters.([36]. Figure 3 (A)-(C) show a schematic diagram of the design process with a frequency-intensity combination (20Hz, 20ma). As shown from the figure, the EMG (Figure 3(A)) produced a lower amplitude than the tc-FES signal (Figure 3(B)). Therefore, the tc-FES-sEMG signal presented a trend similar to the tc-FES signal (Figure 3(C)). This indicates that the EMG is disturbed by FES artifacts. We also obtained the same results under the conditions of other frequency-intensity combinations.

Furthermore, to demonstrate the similarity between the signals of the two channels involving the vEMG, the tc-FES, and the constructed tc-FES-sEMG signals, we plotted several fragments in Figures 3(D)-(F), respectively. As shown, the correlation between the two channels of the vEMG signal was weak, while the correlation between the two channels of the tc-FES signal was high. The results showed that the correlation between the tc-FES-sEMG signal of the two channels was also high, suggesting that the key correlation had been caused by the high similarity between the two tc-FES artifacts. In addition, we plotted the correlation coefficient between two channels of the tc-FES signal, tc-FES-sEMG signal and tc-FES-EMG signal in each condition in Figures 3(G)-(I), respectively. There was high correlation as to whether it happens in the FES signal, FES-sEMG signal or FES-EMG signal ($p>0.98$). This also showed the influence of the FES artifacts in the EMG signal, which provided a prerequisite for the execution of the proposed algorithm.

Preprocessing for the tc-FES-sEMG signa: After constructing simulated EMG data with time constant parameter FES artifacts, we divided the tc-FES-sEMG signals into several non-overlapping segments of 100 data points each using a sliding window approach. Then, we filtered the signals using a 20-200Hz bandpass filter. Subsequently, we applied the G-S-G method to remove FES artifacts. Figures 4 (A)-(C) show the results for frequency-Amplitude combinations of (20 Hz, 10 mA), (20 Hz, 15 mA), and (20 Hz, 20 mA), respectively. As shown in the figure, the proposed G-S-G algorithm effectively removes FES artifacts under different parameters. To demonstrate the superiority of the G-S-G method, we compared it with the 2nd-order G-S-G method in the time domain (2tG-S-G), as presented in Figures 4(D)-(F).

To quantitatively evaluate the performance of our algorithm, we calculated the correlation coefficients and SNR for the 2nd-order G-S algorithm and G-S-G algorithm in the spatial domain, and different orders of the G-S algorithm (ntG-S) and G-S-G algorithm (ntG-S-G) in the time domain. The results are shown in Figures 4 (G)-(J). The results indicate that the multi-channel G-S algorithm outperforms the time-domain G-S algorithm in terms of artifact removal, regardless of whether the subsequent Grubbs' criterion for outlier removal is introduced. Furthermore, the artifact removal effect is more pronounced when the Grubbs' criterion is applied, highlighting the necessity of outlier removal. Additionally, the G-S-G algorithm has a smaller impact on signal quality when stimulus intensity varies, making it more suitable for higher intensity levels.

2) Results for the Tv-FES-sEMG: Furthermore, we constructed the simulation EMG data with time-variate parameter FES artifacts, named tv-FES-sEMG, by fusing the vEMG signals and tv-FES artifacts at a ratio of 1:1. The construction method was the same as the tc-FES-sEMG signal. We randomly selected a fixed tv-FES signal with parameters ranging from 10-30Hz to 10-20mA. Figures 5 (A)-(C) show

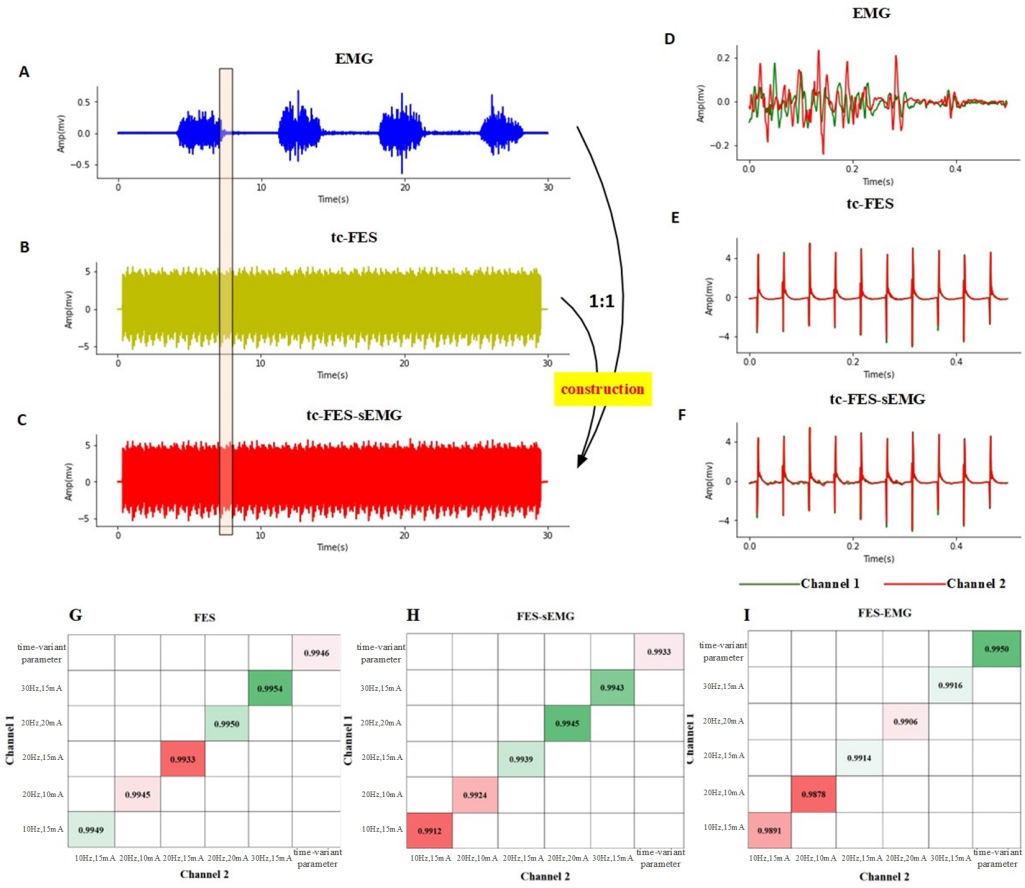

Fig. 3. Construction for simulation EMG data with time-constant parameter FES artifacts. (A)-(C) show a schematic diagram for the construction process with the frequency-intensity combination (20Hz, 20ma). (D)-(F) exhibit the similarity between the two channels' signals for vEMG, tc-FES, and the constructed tc-FES-sEMG signal, respectively. (G)-(I) show the correlation coefficient between two channels of the tc-FES signal, tc-FES-sEMG signal and tc-FES-EMG signal in each condition, respectively.

the vEMG, tv-FES and tv-FES-sEMG signals, respectively. As shown, there is a large artifact in the tv-FES-sEMG signal. After that, we applied the G-S-G method to the tv-FES-sEMG signal and obtained good performance, as shown in Figure 5(D). To examine the preprocessing effect of the G-S-G algorithm, we also calculated the RMS correlation coefficient between the vEMG and the processed tv-FES-sEMG signal (Figure 5(E)). Additionally, we calculated the SNR value of the processed tv-FES-sEMG signal (Figure 5(F)). As shown in Figure 5, the RMS correlation coefficient and SNR values of the processed tv-FES-sEMG signal are larger than traditional time-domain methods, comparable to the results obtained under constant parameters. This demon-strates the effectiveness of the G-S-G method in removing time-varying parameter FES artifacts from EMG signals.

B. Stimulation Artifact Removal for FES-EMG Signals

1) Results for Tc-FES-EMG: Figure 6 shows the experimental data with tc-FES artifacts and the results after applying the G-S-G algorithm for FES artifact removal. Figures 6(A), (B) show the raw tc-FES-EMG signals for 20Hz, 15mA, and 20Hz, 20mA parameters, respectively. Figures 6(C), (D) show the G-S-G algorithm processing results of tc-FES-EMG signals under 20Hz, 15mA, 20Hz, and 20mA parameters, respectively. It can be seen that the proposed G-S-G algorithm also has a good processing effect on the real signal. To quantitatively evaluate the algorithm's performance, we computed the SNR for both the traditional time-domain G-S algorithm and our proposed algorithm, as shown in Figures 6(E), (F). The results demonstrate that our algorithm yields higher SNR values compared to the traditional time-domain G-S algorithm. Moreover, the removal of outliers further enhances the SNR, highlighting the superiority of our algorithm.

2) Results for Tv-FES-EMG: Additionally, we conducted an analysis on the tv-FES-EMG signals with parameters ranging from 10-30Hz and 10-20mA, as depicted in Figure 7. Figure 7 shows the processed results of the tv-FES-EMG signals for both channels. The comprehensive results show that our algorithm also has good performance in processing FES artifacts under time-varying parameters.

IV. Discussions

We have proposed a novel G-S-G method to remove the stimulation artifacts evoked by FES in EMG signals. Our simulated results showed that the G-S-G method was robust to the FES artifacts with varying parameters. Further results showed the algorithm's effectiveness and stability. Furthermore, we applied the proposed method to the experimental EMG data with FES-evoked stimulation artifact, and also achieve good performance. Thus, this study provides a new

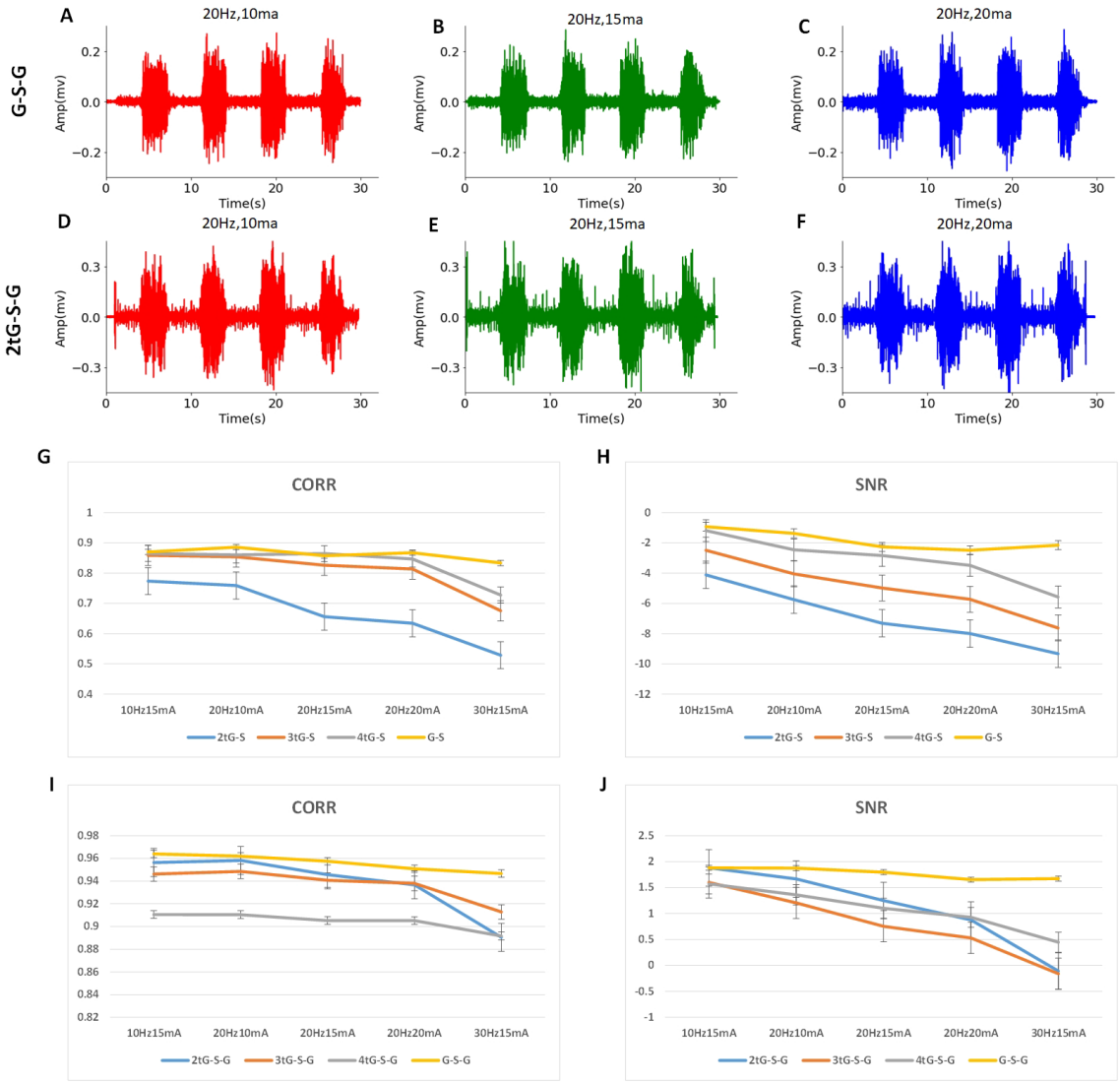

Fig. 4. Results for FES artifact removal. (A)-(C) show the G-S-G results for the frequency-intensity combinations with (20Hz, 10mA), (20Hz, 15mA) and (20Hz, 20mA), respectively. (D)-(F) show the G-S results for the frequency-intensity combinations with (20Hz, 10mA), (20Hz, 15mA) and (20Hz, 20mA), respectively. (G), (I) illustrate the RMS correlation between the vEMG signals and the processed tc-FES-sEMG signals under different algorithms. (H), (J) show the SNR values for the processed tc-FES-sEMG signals under different algorithms.

approach to resolving the problem of removing FES-evoked stimulation artifacts.

A. Existing Necessity of the G-S-G Method

Realizing feedback modulation of FES technology in clinical application is a major challenge [12], [37], [38]. Existing studies have pointed out that EMG signals provide an approach to solving this problem [15], [39], [40]. However, removing the stimulation artifacts in EMG signals remains a challenge, due to the initial spikes and M-waves [17]. Although the amplitude of the stimulation artifact is much higher than that of the EMG signal, in some studies, the blank window method has been applied to remove the artifacts by setting the values of the time period in which FES artifacts dominate to zero [16]. However, when we perform the FES for a long time, the artifacts may also last for several milliseconds, or even tens of milliseconds, which increases the prepressing difficulty [17]. Secondly, the stimulus frequencies of the FES overlap within the EMG signals' frequency ranges [17], [41]. The acquisition device captures both the EMG signals and the FES artifacts. Thus, the two types of data mix. Some researchers have pointed out that the filters and template subtraction methods can remove the artifacts [20], [27]. However, as the muscle fatigues, displacement and other functions change, and the FES artifacts change in shape and amplitude [17], [41]. Each of these factors significantly increase the difficulty of FES artifact removal, and therefore some of the methods are difficult to use on the general population. Thirdly, this will inevitably lead to dynamic changes in stimulation parameters in the process of FES application, and the dynamic changes in FES parameters will further limit the utility of existing algorithms for stimulation artifacts under constant parameters [16]. In addition, to realize the dynamic control of stimulation parameters in FES applications, the algorithm's timeliness must also be satisfied. Thus, algorithm research with

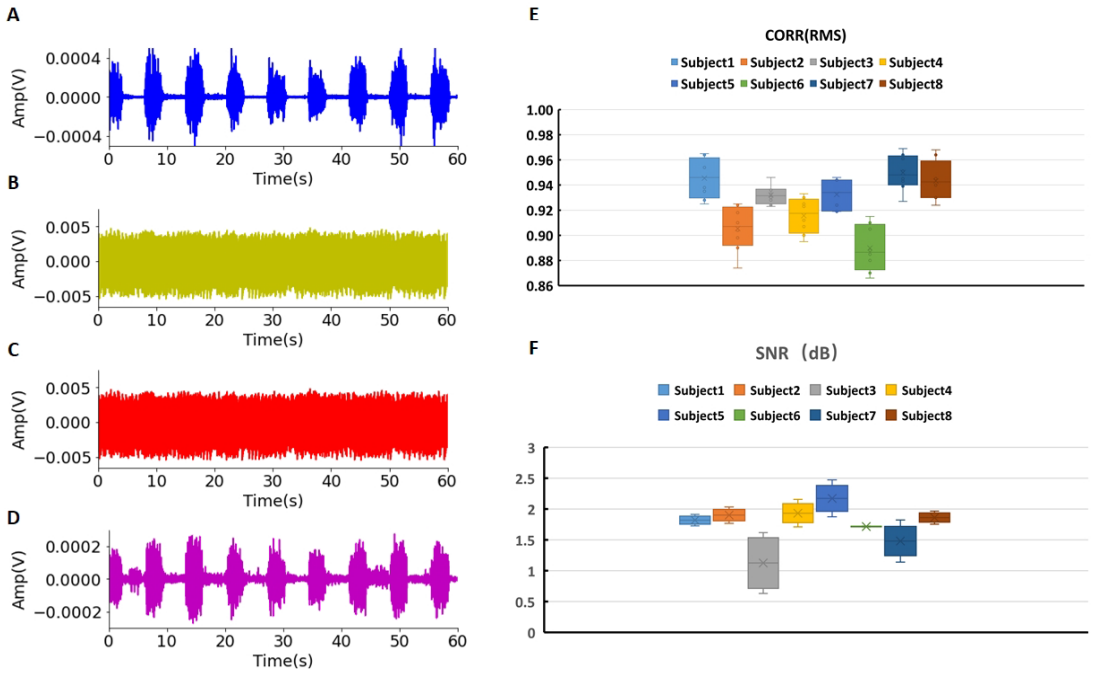

Fig. 5. Results for the tv-FES-sEMG signal. (A)-(D) show the vEMG, tv-FES, tv-FES-sEMG and the tv-FES-sEMG signal after the G-S-G method, respectively. (E) shows the RMS correlation coefficient for each subject under variable parameters. (F) shows the SNR values for each subject.

minimal time consumption and rapid speeds is an inevitable link [28], [42], [43]. Although there are many existing methods for removing artifacts surrounding FES stimulation [21], [44], most of them are implemented for a certain aim. Therefore, it is difficult to achieve dynamic and real-time artifact removal under variable-parameter FES.

Therefore, a new method suitable for real-time analysis of FES artifacts with time-varying parameters is needed. Considering the asynchronicity of EMG recruiting muscles and the synchronicity of FES recruiting muscles [31], [32], we proposed the G-S-G method to suit the artifact removal requirements by fusing the G-S method and Grubbs criterion. This method takes advantage of the correlation and synchronization of stimulus artifacts between channels to remove the M waves and most of the initial peaks. Then, it identifies the remaining initial peaks in the signal as outliers and removes them, so as to eliminate stimulation artifacts and extract vEMG.

B. Merits of the G-S-G Method in FES Artifact Removal

The initial spikes and M-waves are the main inferences for EMG signals during functional electrical stimulation. Previous literature has pointed out that the current methods only can remove one type or part of the FES artifacts, and therefore they are limited in their capacity to eliminate them. For example, the G-S method can remove M waves and most initial spikes [28], and the Grubbs criterion can exclude the initial spikes by identifying any outliers [33]. For this, we fused the G-S method and Grubbs criterion to propose the G-S-G method in this study. Our simulated and experimental results showed good performance of the G-S-G method in removing FES artifacts in EMG signals, especially for M-waves and initial spikes (Figures 6 and Figures 7).

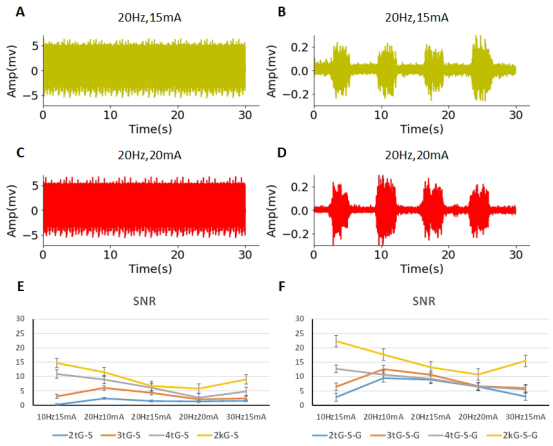

Fig. 6. Results for tc-FES-EMG. (A), (B) show the raw tc-FES-EMG signals under the parameters of 20Hz, 15mA and 20Hz, 20mA, respectively. (C), (D) show the preprocessed tc-FES-EMG signal under the parameters of 20Hz, 15mA, and 20Hz, 20mA, respectively. (E), (F) show the SNR values for the processed tc-FES-sEMG signals under different algorithms.

The template matching method is the mainstream algorithm for effectively removing stimulus artifacts in EMG signals. Most traditional artifact removal methods are implemented using time-domain signals as templates. However, high intensity FES stimulation may cause muscle fatigue, even resulting in changes in the artifact waveform in the time-domain [41]. This results in the difference in the matching between the signal template and the actual output signal. Due to all of these factors, most previous methods have limitations in their ability to remove FES artifacts from EMG signals [15], [22]. In the G-S-G method we proposed, the G-S method and Grubbs criterion are fused, and the main idea of this method is still template matching. In this method, we rely

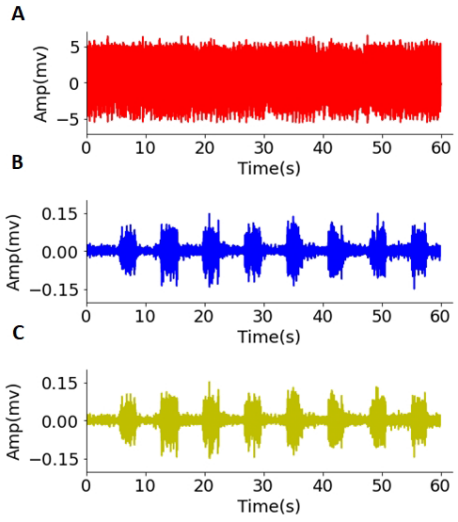

Fig. 7. Results for tv-FES-EMG. (A) shows the raw tv-FES-EMG signal. (B), (C) show the two channels of the preprocessed tv-FES-EMG signal, respectively.

on the high synchronization and correlation of the simulation artifacts among the multi-channel signals within a calculation window [31], so that they can be used as templates for each other. In addition, we introduced a sliding window to divide the signals into several segments, chose the templates, and then calculated the G-S-G in each window. Thus, the template in each window might vary as the FES artifacts change, enabling the G-S-G algorithm to alleviate the problem of template mismatch caused by muscle fatigue, artifact deformation, parameter changes and other factors. Additionally, we introduced a sliding window to split the long data into a series of short segments, which also ensures the G-S-G method's real-time performance [35], [45].

C. Limitations and Future Work

In this study, we have shown that the G-S-G algorithm yields superior performance in removing FES artifacts in EMG signals. However, this method has several limitations. Considering the high synchronization and correlation of the simulation artifacts among the multi-channel signals, we need a high requirement for the placement of the electrodes to achieve the EMG signals. Additionally, when we perform the FES with multiple targets in one muscle, it will cause cross-interference of FES artifacts and reduce the correlation and synchronization between the FES artifacts. This will disable the fixed electrode positioning in our original method, in which case the electrode position will need to be adjusted self-adaptively according to real-time changes in FES artifacts. In future work, we can use high-density EMG electrodes to identify the correlation of FES artifacts between different channels in real-time processing. This can avoid the problem of inflexible positioning of electrodes to a certain extent and improve the signal processing effect.

V. Conclusion

In this study, we have proposed an adaptive spatial filtering algorithm that can extract vEMG with FES artifacts with time-varying parameters. Unlike previous FES-induced stimulation artifact removal algorithms, this G-S-G method targets the synchronicity of vEMG recruiting muscles and the synchronicity of FES-collecting muscles; the signals between channels are analyzed as reference signals from each other. This method overcomes the limitation of FES frequency and amplitude during single-channel EMG preprocessing, realizing the adaptive removal of FES-induced stimulation artifacts under time-varying parameters in multi-channel EMG signals. It also has a good effect on FES-induced stimulation artifacts when the intensity is high. Moreover, the algorithm is simple and has strong real-time performance. Thus, this is a superior method for application to FES-induced stimulation artifact removal under time-varying parameters in multi-channel EMG signals.

Appendix

We have added a video about the real-time removal of the FES artifacts from raw EMG in appendix I, and also added the key codes of our proposed algorithm in appendix II.

Acknowledgment

The authors would like to thank the editor and reviewers for their helpful comments which have improved this manuscript.

References

[1] C. Marquez-Chin and M. R. Popovic, "Functional electrical stimulation therapy for restoration of motor function after spinal cord injury and stroke: A review," *Biomed. Eng. OnLine*, vol. 19, no. 1, pp. 1–12, May 2020, doi: 10.1186/s12938-020-00773-4.

[2] R. G. Carson and A. R. Buick, "Neuromuscular electrical stimulation-promoted plasticity of the human brain," *J. Physiol.*, vol. 599, no. 9, pp. 2375–2399, May 2021, doi: 10.1113/jp278298.

[3] B. A. Karamian et al., "The role of electrical stimulation for rehabilitation and regeneration after spinal cord injury," *J. Orthopaedics Traumatol.*, vol. 23, no. 1, pp. 1–20, Dec. 2022, doi: 10.1186/s10195-021-00623-6.

[4] G. E. Kang et al., "The effect of implanted functional electrical stimulation on gait performance in stroke survivors: A systematic review," *Sensors*, vol. 21, no. 24, p. 8323, Dec. 2021, doi: 10.3390/s21248323.

[5] F. Quandt and F. C. Hummel, "The influence of functional electrical stimulation on hand motor recovery in stroke patients: A review," *Experim. Transl. Stroke Med.*, vol. 6, no. 1, pp. 1–11, Dec. 2014, doi: 10.1186/2040-7378-6-9.

[6] J. Chae, Z. P. Fang, M. Walker, and S. Pourmehdi, "Intramuscular electromyographically controlled neuromuscular electrical stimulation for upper limb recovery in chronic hemiplegia," *Amer. J. Phys. Med. Rehabil.*, vol. 80, no. 12, pp. 935–941, Dec. 2001, doi: 10.1097/00002060-200112000-00011.

[7] Y. Hara, S. Ogawa, and Y. Muraoka, "Hybrid power-assisted functional electrical stimulation to improve hemiparetic upper-extremity function," *Amer. J. Phys. Med. Rehabil.*, vol. 85, no. 12, pp. 977–985, Dec. 2006, doi: 10.1097/01.phm.0000247853.61055.f8.

[8] Z. Li, D. Guiraud, D. Andreu, A. Gelis, C. Fattal, and M. Hayashibe, "Real-time closed-loop functional electrical stimulation control of muscle activation with evoked electromyography feedback for spinal cord injured patients," *Int. J. Neural Syst.*, vol. 28, no. 6, Aug. 2018, Art. no. 1750063, doi: 10.1142/s0129065717500630.

[9] M. Crepaldi et al., "FITFES: A wearable myoelectrically controlled functional electrical stimulator designed using a user-centered approach," *IEEE Trans. Neural Syst. Rehabil. Eng.*, vol. 29, pp. 2142–2152, 2021, doi: 10.1109/TNSRE.2021.3120293.

[10] D. Andreu, B. Sijobert, M. Toussaint, C. Fattal, C. Azevedo-Coste, and D. Guiraud, "Wireless electrical stimulators and sensors network for closed loop control in rehabilitation," *Frontiers Neurosci.*, vol. 14, p. 117, Feb. 2020, doi: 10.3389/fnins.2020.00117.

[11] Y.-X. Zhou, H.-P. Wang, X.-L. Bao, X.-Y. Lü, and Z.-G. Wang, "A frequency and pulse-width co-modulation strategy for transcutaneous neuromuscular electrical stimulation based on sEMG time-domain features," *J. Neural Eng.*, vol. 13, no. 1, Feb. 2016, Art. no. 016004, doi: 10.1088/1741-2560/13/1/016004.

[12] F. Medina, K. Perez, D. Cruz-Ortiz, M. Ballesteros, and I. Chairez, "Control of a hybrid upper-limb orthosis device based on a data-driven artificial neural network classifier of electromyography signals," *Biomed. Signal Process. Control*, vol. 68, Jul. 2021, Art. no. 102624, doi: 10.1016/j.bspc.2021.102624.

[13] B. A. Hasse, D. E. G. Sheets, N. L. Holly, K. M. Gothard, and A. J. Fuglevand, "Restoration of complex movement in the paralyzed upper limb," *J. Neural Eng.*, vol. 19, no. 4, Aug. 2022, Art. no. 046002, doi: 10.1088/1741-2552/ac7ad7.

[14] S. Sa-e, C. T. Freeman, and K. Yang, "Iterative learning control of functional electrical stimulation in the presence of voluntary user effort," *Control Eng. Pract.*, vol. 96, Mar. 2020, Art. no. 104303, doi: 10.1016/j.conengprac.2020.104303.

[15] B. A. C. Osuagwu, E. Whicher, and R. Shirley, "Active proportional electromyogram controlled functional electrical stimulation system," *Sci. Rep.*, vol. 10, no. 1, p. 21242, Dec. 2020, doi: 10.1038/s41598-020-77664-0.

[16] S. Sennels, F. Biering-Sorensen, O. T. Andersen, and S. D. Hansen, "Functional neuromuscular stimulation controlled by surface electromyographic signals produced by volitional activation of the same muscle: Adaptive removal of the muscle response from the recorded EMG-signal," *IEEE Trans. Rehabil. Eng.*, vol. 5, no. 2, pp. 195–206, Jun. 1997, doi: 10.1109/86.593293.

[17] F. Mandrile, D. Farina, M. Pozzo, and R. Merletti, "Stimulation artifact in surface EMG signal: Effect of the stimulation waveform, detection system, and current amplitude using hybrid stimulation technique," *IEEE Trans. Neural Syst. Rehabil. Eng.*, vol. 11, no. 4, pp. 407–415, Dec. 2003, doi: 10.1109/TNSRE.2003.819791.

[18] Y. Muraoka, "Development of an EMG recording device from stimulation electrodes for functional electrical stimulation," *Frontiers Med. Biol. Eng., Int. J. Jpn. Soc. Med. Electron. Biol. Eng.*, vol. 11, no. 4, pp. 323–333, 2002, doi: 10.1163/156855701321138969.

[19] C. Frigo, M. Ferrarin, W. Frasson, E. Pavan, and R. Thorsen, "EMG signals detection and processing for on-line control of functional electrical stimulation," *J. Electromyogr. Kinesiol., Off. J. Int. Soc. Electrophysiolog. Kinesiol.*, vol. 10, no. 5, pp. 351–360, Oct. 2000, doi: 10.1016/s1050-6411(00)00026-2.

[20] E. Langzam, E. Isakov, and J. Mizrahi, "Evaluation of methods for extraction of the volitional EMG in dynamic hybrid muscle activation," *J. NeuroEng. Rehabil.*, vol. 3, no. 1, p. 27, Nov. 2006, doi: 10.1186/1743-0003-3-27.

[21] D. T. O'Keeffe, G. M. Lyons, A. E. Donnelly, and C. A. Byrne, "Stimulus artifact removal using a software-based two-stage peak detection algorithm," *J. Neurosci. Methods*, vol. 109, no. 2, pp. 137–145, Aug. 2001, doi: 10.1016/s0165-0270(01)00407-1.

[22] K. Limnuson, H. Lu, H. J. Chiel, and P. Mohseni, "Real-time stimulus artifact rejection via template subtraction," *IEEE Trans. Biomed. Circuits Syst.*, vol. 8, no. 3, pp. 391–400, Jun. 2014, doi: 10.1109/TBCAS.2013.2274574.

[23] R. Pilkar et al., "Application of empirical mode decomposition combined with notch filtering for interpretation of surface electromyograms during functional electrical stimulation," *IEEE Trans. Neural Syst. Rehabil. Eng.*, vol. 25, no. 8, pp. 1268–1277, Aug. 2017, doi: 10.1109/TNSRE.2016.2624763.

[24] E. R. de Lima, A. O. Andrade, J. L. Pons, P. Kyberd, and S. J. Nasuto, "Empirical mode decomposition: A novel technique for the study of tremor time series," *Med. Biol. Eng. Comput.*, vol. 44, no. 7, pp. 569–582, Jul. 2006, doi: 10.1007/s11517-006-0065-x.

[25] R. Thorsen, R. Spadone, and M. Ferrarin, "A pilot study of myoelectrically controlled FES of upper extremity," *IEEE Trans. Neural Syst. Rehabil. Eng.*, vol. 9, no. 2, pp. 161–168, Jun. 2001, doi: 10.1109/7333.928576.

[26] Y. Zhou et al., "A data-driven volitional EMG extraction algorithm during functional electrical stimulation with time variant parameters," *IEEE Trans. Neural Syst. Rehabil. Eng.*, vol. 28, no. 5, pp. 1069–1080, May 2020, doi: 10.1109/TNSRE.2020.2980294.

[27] Y. Li, J. Chen, and Y. Yang, "A method for suppressing electrical stimulation artifacts from electromyography," *Int. J. Neural Syst.*, vol. 29, no. 6, Aug. 2019, Art. no. 1850054, doi: 10.1142/s0129065718500545.

[28] H. Yeom and Y.-H. Chang, "Autogenic EMG-controlled functional electrical stimulation for ankle dorsiflexion control," *J. Neurosci. Methods*, vol. 193, no. 1, pp. 118–125, Oct. 2010, doi: 10.1016/j.jneumeth.2010.08.011.

[29] R. C. Oldfield, "The assessment and analysis of handedness: The Edinburgh inventory," *Neuropsychologia*, vol. 9, no. 1, pp. 97–113, Mar. 1971.

[30] S. Pizzolato, L. Tagliapietra, M. Cognolato, M. Reggiani, H. Müller, and M. Atzori, "Comparison of six electromyography acquisition setups on hand movement classification tasks," *PLoS ONE*, vol. 12, no. 10, Oct. 2017, Art. no. e0186132, doi: 10.1371/journal.pone.0186132.

[31] C. S. Bickel, C. M. Gregory, and J. C. Dean, "Motor unit recruitment during neuromuscular electrical stimulation: A critical appraisal," *Eur. J. Appl. Physiol.*, vol. 111, no. 10, pp. 2399–2407, Oct. 2011, doi: 10.1007/s00421-011-2128-4.

[32] C. J. De Luca, "Physiology and mathematics of myoelectric signals," *IEEE Trans. Bio-Med. Eng.*, vol. BME-26, no. 6, pp. 313–325, Jun. 1979, doi: 10.1109/TBME.1979.326534.

[33] J. N. Miller, "Using the Grubbs and Cochran tests to identify outliers," *Anal. Methods*, vol. 7, no. 19, pp. 7948–7950, 2015, doi: 10.1039/c5ay90053k.

[34] Z. Zhang, K. Yang, J. Qian, and L. Zhang, "Real-time surface EMG pattern recognition for hand gestures based on an artificial neural network," *Sensors*, vol. 19, no. 14, p. 3170, Jul. 2019, doi: 10.3390/s19143170.

[35] K. Momen, S. Krishnan, and T. Chau, "Real-time classification of forearm electromyographic signals corresponding to user-selected intentional movements for multifunction prosthesis control," *IEEE Trans. Neural Syst. Rehabil. Eng.*, vol. 15, no. 4, pp. 535–542, Dec. 2007, doi: 10.1109/TNSRE.2007.908376.

[36] S. Qiu et al., "A stimulus artifact removal technique for SEMG signal processing during functional electrical stimulation," *IEEE Trans. Biomed. Eng.*, vol. 62, no. 8, pp. 1959–1968, Aug. 2015, doi: 10.1109/TBME.2015.2407834.

[37] J. S. Knutson et al., "Adding contralaterally controlled electrical stimulation of the triceps to contralaterally controlled functional electrical stimulation of the finger extensors reduces upper limb impairment and improves reachable workspace but not dexterity: A randomized controlled trial," *Amer. J. Phys. Med. Rehabil.*, vol. 99, no. 6, pp. 514–521, Jun. 2020, doi: 10.1097/phm.0000000000001363.

[38] Z. Li, D. Guiraud, D. Andreu, C. Fattal, A. Gelis, and M. Hayashibe, "A hybrid functional electrical stimulation for real-time estimation of joint torque and closed-loop control of muscle activation," *Eur. J. Transl. Myol.*, vol. 26, no. 3, p. 6064, Jun. 2016.

[39] Q. Zhang, M. Hayashibe, and C. Azevedo-Coste, "Evoked electromyography-based closed-loop torque control in functional electrical stimulation," *IEEE Trans. Biomed. Eng.*, vol. 60, no. 8, pp. 2299–2307, Aug. 2013, doi: 10.1109/TBME.2013.2253777.

[40] J. P. Giuffrida and P. E. Crago, "Reciprocal EMG control of elbow extension by FES," *IEEE Trans. Neural Syst. Rehabil. Eng.*, vol. 9, no. 4, pp. 338–345, Dec. 2001, doi: 10.1109/7333.1000113.

[41] R. Merletti, M. Knaflitz, and C. J. DeLuca, "Electrically evoked myoelectric signals," *Crit. Rev. Biomed. Eng.*, vol. 19, no. 4, pp. 293–340, 1992.

[42] X. Yi, J. Jia, S. Deng, S. G. Shen, Q. Xie, and G. Wang, "A blink restoration system with contralateral EMG triggered stimulation and real-time artifact blanking," *IEEE Trans. Biomed. Circuits Syst.*, vol. 7, no. 2, pp. 140–148, Apr. 2013, doi: 10.1109/TBCAS.2013.2255051.

[43] G. Hefftner, W. Zucchini, and G. G. Jaros, "The electromyogram (EMG) as a control signal for functional neuromuscular stimulation—Part I: Autoregressive modeling as a means of EMG signature discrimination," *IEEE Trans. Bio-Med. Eng.*, vol. BME-35, no. 4, pp. 230–237, Apr. 1988, doi: 10.1109/10.1370.

[44] A. Dutta, R. Kobetic, and R. J. Triolo, "Ambulation after incomplete spinal cord injury with EMG-triggered functional electrical stimulation," *IEEE Trans. Biomed. Eng.*, vol. 55, no. 2, pp. 791–794, Feb. 2008, doi: 10.1109/TBME.2007.902225.

[45] T. Tanaka, I. Nambu, Y. Maruyama, and Y. Wada, "Sliding-window normalization to improve the performance of machine-learning models for real-time motion prediction using electromyography," *Sensors*, vol. 22, no. 13, p. 5005, Jul. 2022, doi: 10.3390/s22135005.